

Neural Networks for Navigation: From Connections to Computations

Rachel I. Wilson

Department of Neurobiology, Harvard Medical School, Cambridge, Massachusetts, USA;
email: rachel_wilson@hms.harvard.edu

Annu. Rev. Neurosci. 2023. 46:403–23

The *Annual Review of Neuroscience* is online at
neuro.annualreviews.org

<https://doi.org/10.1146/annurev-neuro-110920-032645>

Copyright © 2023 by the author(s). This work is licensed under a Creative Commons Attribution 4.0 International License, which permits unrestricted use, distribution, and reproduction in any medium, provided the original author and source are credited. See credit lines of images or other third-party material in this article for license information.

**ANNUAL
REVIEWS CONNECT**

www.annualreviews.org

- Download figures
- Navigate cited references
- Keyword search
- Explore related articles
- Share via email or social media

Keywords

memory, menotaxis, path integration, head direction, dopamine, coordinate transformation

Abstract

Many animals can navigate toward a goal they cannot see based on an internal representation of that goal in the brain's spatial maps. These maps are organized around networks with stable fixed-point dynamics (attractors), anchored to landmarks, and reciprocally connected to motor control. This review summarizes recent progress in understanding these networks, focusing on studies in arthropods. One factor driving recent progress is the availability of the *Drosophila* connectome; however, it is increasingly clear that navigation depends on ongoing synaptic plasticity in these networks. Functional synapses appear to be continually reselected from the set of anatomical potential synapses based on the interaction of Hebbian learning rules, sensory feedback, attractor dynamics, and neuromodulation. This can explain how the brain's maps of space are rapidly updated; it may also explain how the brain can initialize goals as stable fixed points for navigation.

Contents

INTRODUCTION	404
ORIENTATION	406
EVIDENCE INTEGRATION	407
PLASTICITY	408
LEARNING AT THE RIGHT TIME	409
BEYOND HEAD DIRECTION	411
STEERING	412
SELECTING AND STORING A GOAL	414
TRANSLATIONAL VELOCITY	414
PATH INTEGRATION	416
OUTLOOK	417

INTRODUCTION

It is in his moment of hesitation that you sense him as an intelligent creature. Between his pause and his change of direction, you are sure, there is a quick thought.

—Lydia Davis, “Cockroaches in Autumn”

If we could see all the arthropods in the world at the same time, we would see more than a quintillion bodies in motion, each pursuing its own goal. We might see a butterfly taking off on a migratory flight, an ant setting out for its underground nest, a shrimp returning to its distant burrow, or a bee winging its way toward a far-off meadow. In each of these examples, the organism cannot see or otherwise perceive its intended goal. Instead, the goal location must be written into memory, referenced to external landmarks and compass cues, and read out for continuous navigation control.

Inside the arthropod brain, the neural networks that guide internally directed navigation are collectively termed the central complex. These networks reside at the midline of the central brain (**Figure 1a**), and they are so distinctive that they have been called the brain within the brain (Strausfeld 2012). They compute a running estimate of the organism’s state—its orientation, position, rotational velocity, and translational velocity—by integrating multiple streams of evidence, performing a series of spatial coordinate transformations, and building an internal map of the external world. These networks may also generate and store some of the policies that trigger appropriate motor commands based on the organism’s current state.

Some features of the central complex are clearly analogous to features of primate and rodent brains; the head direction system is a clear example of this. At the same time, the arthropod central complex has much in common with the control system of an autonomous robot or a very small self-driving car: It should be completely explainable in mechanistic terms using concepts from dynamical systems and control theory. Thus, arthropod brains occupy an uncanny middle ground between human brains and artificial intelligence. Moreover, the first complete neural wiring diagram (connectome) of a complex organism will come from an arthropod—namely, *Drosophila melanogaster*, whose central nervous system comprises about 150,000 neurons (Bates et al. 2019). It turns out that the anatomical wiring of the *Drosophila* brain is remarkably similar in different individuals (Schlegel et al. 2021). Moreover, many neurons in the *Drosophila* connectome are uniquely identifiable based on their morphology, and they can be targeted for in vivo electrophysiology or

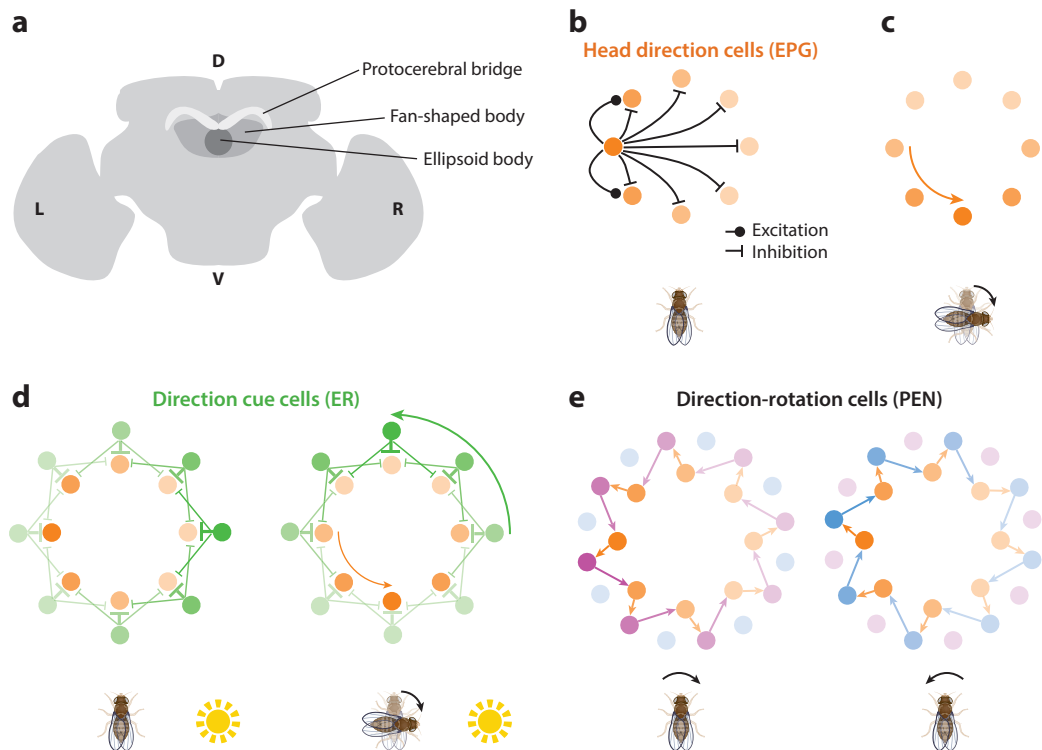


Figure 1

A topographic map of head direction. (a) Key divisions of the central complex in the *Drosophila* brain. Analogous structures are found in other arthropods (Honkanen et al. 2019). Here and elsewhere, the brain is shown from the posterior side, with D/V/L/R denoting dorsal/ventral/left/right. (b) Local excitation and global inhibition maintain a focal bump of activity in the network of primary head direction cells. In *Drosophila*, these are called EPG neurons, and their dendrites are arranged in a circle in the ellipsoid body. Darker shading denotes higher neural activity. The mapping from head directions to neurons is arbitrary and flexible. (c) As the organism turns right, the bump of activity moves counterclockwise (as viewed from the posterior side). (d) The activity bump in EPG neurons is steered around the circle by inhibitory input from direction cue cells (ER neurons). If the environment contains a single bright visual cue (e.g., the sun), this will activate a few adjacent ER neurons, which then push the bump away from the EPG population that they target. When the organism turns right, the image of the cue moves leftward across its retina, causing the bump of activity in ER neurons to rotate counterclockwise. (e) Direction-rotation cells (PEN neurons) receive input from EPG neurons, and they form a pair of secondary head direction maps. One PEN population is active when the organism rotates right (*magenta*), while the other is active when the organism rotates left (*blue*). Because direction-rotation cells send shifted projections back to EPG neurons, any asymmetry in the overall level of activity in the two PEN populations will push the bump of activity around the EPG head direction map.

imaging using specific transgenic lines. Thus, the connectome allows us to generate testable ideas about how specific computations might actually be implemented by biological neural networks.

In what follows, I will summarize recent work on the central complex networks for navigation in *Drosophila* and other arthropods. The central complex is conserved across arthropods (Honkanen et al. 2019, Strausfeld 2012, Thoen et al. 2017), and the basic modules of navigation behavior are also conserved (Dickinson 2014), so we can learn a great deal by synthesizing data from different arthropod species. That said, arthropods are also diverse, and so I must apologize in advance for not drawing attention to the specializations of different species, as my aim here is to extract general principles.

Much of the recent work on the arthropod central complex is guided by connectome data, but I also argue that we should not take the connectome too literally, because some of these anatomical

synapses seem to be functionally silent. I suggest that the set of functional synapses (the functional connectome) is constantly in flux, and it is shaped by the interaction of Hebbian plasticity with sensory feedback, attractor dynamics, and neuromodulation. These processes align the organism's motor commands with its current goal; when the environment changes, the functional connectome is rapidly reorganized. Similarly, when the organism needs to change its goal, the functional connectome may also be reorganized. These mechanisms provide a way to implement rapid read/write memory in a dynamical neural network.

ORIENTATION

A system of interconnected topographic maps of head direction lie at the core of the navigation networks in the arthropod brain (Honkanen et al. 2019, Hulse & Jayaraman 2020). This system has many similarities to the mammalian head direction system, noted years ago (Homberg 2004, Labhart & Meyer 2002, Sakura et al. 2008). In both arthropods and mammals, there are multiple sets of head direction cells with correlated dynamics (Green et al. 2017, Heinze & Homberg 2007, Taube 1995, Taube et al. 1990a, Turner-Evans et al. 2017). Individual head direction cells are narrowly tuned, and they collectively tile the space of compass directions (Ajabi et al. 2021, Heinze & Homberg 2007, Seelig & Jayaraman 2015). Moreover, in both arthropods and mammals, head direction cells are sensitive to multimodal cues (Okubo et al. 2020, Pfeiffer & Homberg 2007, Taube et al. 1990b), and the mapping from directions to neurons is flexible and seemingly arbitrary (Heinze & Homberg 2009, Seelig & Jayaraman 2015, Taube et al. 1990b). Importantly, the head direction system can function even in the absence of any external landmarks by integrating rotational velocity cues over time (Green et al. 2017, Mizumori & Williams 1993, Seelig & Jayaraman 2015, Taube et al. 1990b, Turner-Evans et al. 2017). In mammals, these rotational velocity cues originate in the vestibular system, whereas in arthropods, they probably arise from the proprioceptive system, as well as motor efference copy.

Both the arthropod and mammalian head direction systems function as ring attractors, that is, networks that use persistent activity to store the value of a circular variable (Knierim & Zhang 2012). In arthropods, the head direction system is topographic (Heinze & Homberg 2007, Seelig & Jayaraman 2015), so persistent activity appears as a stable bump in the network of primary head direction cells, called EPG neurons (**Figure 1b,c**).¹ Persistent activity is likely due to the excitatory connections between EPG neurons with overlapping direction preferences (Hulse et al. 2021, Turner-Evans et al. 2020). Meanwhile, global lateral inhibition restricts the activity in each map to a few adjacent EPG neurons (Franconville et al. 2018, Kim et al. 2017). Adjacent EPG neurons receive similar patterns of input from cells that encode the position of direction cues in the environment (Fisher et al. 2019) (**Figure 1d**). Many of these direction cue cells are tuned to solar direction cues—for example, the position of the sun in the sky or patterns of polarized sunlight which rotate as the sun moves (Honkanen et al. 2019). When these sorts of direction cues are available, they exert a strong influence on EPG neurons (Heinze & Homberg 2007, Seelig & Jayaraman 2015).

When direction cues are lacking, rotational velocity cues can still push the bump of activity around the map. This effect reflects the contribution of direction-rotation cells (PEN neurons), which are conjunctively tuned to head direction and rotational velocity (Green et al. 2017, Turner-Evans et al. 2017). These direction-rotation cells form a pair of head direction maps: One is active when the organism rotates right, while the other is active when the organism rotates left

¹This review follows the latest convention for *Drosophila* cell type names (Hulse et al. 2021). All these cell types have different names in other arthropod species (Honkanen et al. 2019).

(Figure 1e). Direction-rotation cells send shifted projections back to the primary (EPG) map, and so any asymmetry in their activity will push the bump of activity around all three maps in a concerted manner. This architecture corresponds well to previous theoretical predictions regarding the mechanisms of rotational velocity integration (Skaggs et al. 1995, Zhang 1996). The experimental data supporting this model come from *Drosophila*; there are discrepant data in locusts (Heinze & Homberg 2007), but more work is needed to understand this discrepancy.

It makes sense that the head direction system should combine direction cues and rotational velocity cues because these two types of cues have complementary virtues. The virtue of rotational velocity cues is that they are always available—unlike direction cues, which may be unavailable in darkness or in barren environments. The problem with rotational velocity cues is that they cannot support an accurate head direction estimate for very long. When rotational velocity cues are integrated over time, the noise or error associated with these inputs accumulates (Cheng et al. 2007, Kutschireiter et al. 2022). Thus, for example, when we close our eyes, we can briefly maintain our sense of direction by tracking our rotational movements, but we progressively lose our bearings as we move. Like a clock that runs fast or slow, we need frequent resets to remain accurate, and this is what direction cues provide. Of course, this reset may not always be accurate in an environment where different gaze directions look similar (Beetz et al. 2021, Fisher et al. 2019, Haberkern et al. 2022, Kim et al. 2019), but rotational velocity cues can help solve this problem: Our ability to track our rotational movements prevents us from becoming immediately disoriented in an environment with rotational symmetry, like a tunnel. Rotational velocity cues also serve to instruct Hebbian plasticity at synapses from direction cue cells onto head direction cells (Fisher et al. 2019, Kim et al. 2019); we return to this topic below.

EVIDENCE INTEGRATION

The brain's head direction estimate depends mainly on input from direction cue cells, called ER neurons. Some ER neurons respond robustly to isolated bright objects that resemble the sun (Omoto et al. 2017, Seelig & Jayaraman 2013, Sun et al. 2017). In these ER neurons, selectivity for the sun (versus other bright objects) may be reinforced by spectral cues (el Jundi et al. 2015a, Pfeiffer & Homberg 2007). Meanwhile, other ER neurons respond to patterns of polarized sunlight, which also provide information about the sun's position (Hardcastle et al. 2021). In some insects, individual ER-like neurons respond to both a bright object and a particular polarization pattern (el Jundi et al. 2015b, Heinze & Reppert 2011, Pegel et al. 2018, Pfeiffer et al. 2005); these cells may use both sets of cues to obtain a better estimate of the sun's position. It makes sense that we should find many ER neurons tuned to the sun's position, as behavioral studies have emphasized the importance of solar cues for menotaxis—that is, navigating in a straight line in an arbitrary direction (Dacke et al. 2021, Homberg 2015, Warren et al. 2019). Some arthropods also use the moon or a prominent constellation of stars for a similar purpose (Dacke et al. 2004, 2013; Ugolini & Chiussi 1996), and in doing so, they may rely on the same ER neurons.

Notably, walking arthropods can also use the wind as a directional cue for menotaxis, relying on mechanosensors to detect the direction of the prevailing wind (Bell & Kramer 1979, Böhm 1995, Böhm et al. 1991, Dacke et al. 2019, Heinzel & Böhm 1989, Müller & Wehner 2007).² Note that wind-guided menotaxis is distinct from simple upwind or downwind walking: In menotaxis, the organism is adopting an arbitrary bearing relative to the wind because it is aiming for a distant or remembered location, and the wind simply happens to be a useful directional cue. Given that

²Flying animals cannot detect wind direction using mechanosensors (Schöne 2014); instead, they rely on optic flow (van Breugel et al. 2022), but we do not know if the head direction system has access to this information.

menotaxis requires the head direction system, we would predict that head direction estimates can be influenced by the wind, and indeed this prediction was confirmed by recent work in *Drosophila*, which also discovered a novel type of ER neuron which encodes wind direction (Okubo et al. 2020). Finally, there might also be ER neurons that are sensitive to magnetic fields, given that some arthropods use the Earth's magnetic field to guide menotaxis (Arendse & Kruyswijk 1981, Boles & Lohmann 2003, Fleischmann et al. 2018).

The integration of multiple direction cues and rotational velocity cues is what allows navigation to proceed seamlessly even when one cue drops out (Dacke et al. 2019, el Jundi et al. 2016, Green et al. 2017, Müller & Wehner 2007, Seelig & Jayaraman 2015). However, the availability of multiple cues introduces several new problems. First, cues should be ideally weighted according to their reliability. Second, the relationship between the sun's position and the wind direction needs to be learned. The relationship between the sun's image and the solar polarization pattern also needs to be learned in some arthropods (el Jundi et al. 2016). As we will see below, synaptic plasticity may be part of the brain's solution to both problems.

PLASTICITY

Curiously, the connectome shows that each ER neuron makes anatomical synapses onto every EPG neuron without any systematic anatomical heterogeneities (Hulse et al. 2021) (**Figure 2a**). ER→EPG synapses are inhibitory, and so if all of these anatomical synapses were actually functional, then each EPG neuron would be hyperpolarized for every head direction. However, whole-cell recordings demonstrate that each EPG neuron has a spatially restricted visual receptive field (Fisher et al. 2019), with adjacent EPG neurons having adjacent receptive fields (**Figure 2b**). As expected, these visual responses are inhibitory. Notably, when the environment is altered, it causes a rapid relearning of the spatial pattern of head direction–evoked inhibition in EPG neurons. Specifically, from the perspective of an individual EPG neuron, visually evoked inhibition

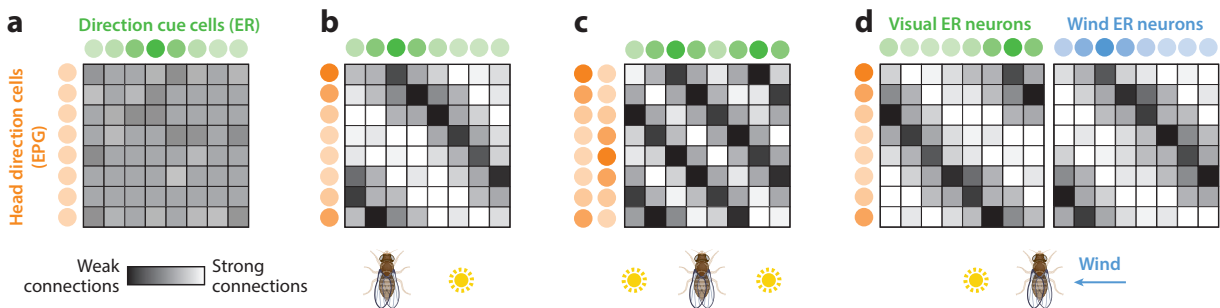


Figure 2

Learning a directional map. (a) ER→EPG connections are anatomically fairly uniform. If all of these inhibitory connections were functional, then the EPG population would be uniformly inhibited by a directional cue. (b) Functional connections are nonuniform. In a familiar virtual environment with one distant visual cue (a virtual sun), each EPG neuron is inhibited by a restricted range of cue positions. When an ER neuron is active, it pushes the EPG bump to the region where its inhibitory output is minimal. (c) In an environment with two identical virtual suns on opposite sides of the environment, the ER→EPG weight map rapidly rearranges to reflect the altered correlation between rotational movement and visual feedback. The bump of EPG activity now toggles between two coordinate frames. After returning to the one-sun environment, the bump of EPG activity continues to toggle for a few minutes, consistent with the idea that ER→EPG connections have been altered. (d) In an environment with multiple types of cues, we might hypothesize that synaptic weights rearrange via Hebbian plasticity, so that the angular separation between the cues is reflected in the spatial phase shift in the weight matrices. For example, if the sun is in the west and the wind is blowing from the east, we might expect a 180° offset in the weights of visual ER neurons and wind ER neurons. Matrices are simplified schematics based on data and computational models from Fisher et al. (2019, 2022), Hulse et al. (2021), and Kim et al. (2019).

is depressed for some head directions and potentiated for others, implying bidirectional changes in the strength of ER→EPG synapses (Fisher et al. 2019) (**Figure 2c**). More evidence for associative plasticity at ER→EPG synapses comes from perturbation experiments (Kim et al. 2019). Here, a focal optogenetic stimulus is used to create an artificial EPG bump with a new arbitrary angular offset from a visual cue. If the bump and the cue are paired with the same systematic offset for all cue positions, then this bump-cue relationship persists even after the optogenetic stimulus is terminated. Together, these recent experimental results confirm the long-standing theoretical prediction that sensory inputs to head direction cells should be plastic (Cope et al. 2017, Page et al. 2014, Skaggs et al. 1995).

Specifically, these results suggest a model where correlated pre- and postsynaptic activity triggers associative long-term synaptic depression at ER→EPG synapses. When an individual ER neuron is activated by a cue, it tends to push the bump of activity toward the EPG neurons it most weakly inhibits (**Figure 2b**). This then produces long-term depression, causing the weakest output synapses of that ER neuron to become even weaker. This learning rule is Hebbian because it reinforces the influence of the neurons that are already most influential; the twist here is that influence is mediated by disinhibition rather than excitation. To ensure network stability, associative long-term depression may be balanced by nonassociative long-term potentiation.

Importantly, plasticity in this system is rapid: Weights can be reorganized within a few minutes after a change in the environmental cue configuration (Fisher et al. 2019, Kim et al. 2019). This type of rapid plasticity can account for why the EPG bump has an idiosyncratic offset relative to the sun or wind (Heinze & Homberg 2009, Okubo et al. 2020, Seelig & Jayaraman 2015): This offset probably just reflects the position that the bump happened to be in when the fly was first exposed to the current cue configuration, as rapid plasticity tends to stabilize that offset.

Notably, Hebbian plasticity provides a potential mechanism for reliability-weighted evidence accumulation: Cues that are reliable indicators of heading are highly correlated with the brain's internal estimate of head direction, and thus the influence of these cues should be boosted over time. Hebbian plasticity also provides a potential mechanism for cue configuration learning (Dacke et al. 2019, el Jundi et al. 2016, Müller & Wehner 2007). Specifically, we might hypothesize that the current pattern of ER→EPG weights represents a stored internal model of the reliable direction cues in the environment and their relative positions (**Figure 2d**), based on the organism's recent experience.

In short, recent studies demonstrate that the arthropod head direction network has two distinct read/write memory mechanisms operating on similar timescales. On one hand, the persistent activity of the ring attractor stores the current head direction estimate. On the other hand, Hebbian plasticity at sensory synapses stores an internal model of the environment. The internal model of the environment is read out to update the current head direction estimate, while the current head direction estimate is read out to update the brain's internal model of the environment.

LEARNING AT THE RIGHT TIME

Rapid plasticity can be potentially destructive because stored information can be easily corrupted. For this reason, in artificial neural networks, learning is generally restricted to specific training epochs. During training, the network is presented with rich statistical data; then connections are frozen outside of these training epochs to prevent the loss of stored information (Rumelhart et al. 1986). In biological networks, a similar sort of strategy could be implemented by invoking a when-to-learn signal that indicates when synapses should be eligible for plasticity (Frémaux & Gerstner 2015). For example, in mammals, some dopamine neurons are selectively activated by reward prediction errors, and dopamine release promotes reward learning in response to these errors

(Watabe-Uchida et al. 2017). In the *Drosophila* mushroom body, dopamine promotes bidirectional synaptic plasticity (Cohn et al. 2015, Handler et al. 2019, Hige et al. 2015).

Notably, there is new evidence that dopamine also serves as a when-to-learn signal governing plasticity in the *Drosophila* head direction system. Specific dopaminergic neurons target the *Drosophila* head direction network (Grover et al. 2022, Liang et al. 2019), and they are selectively active when the fly turns. Indeed, the activity of these dopamine neurons scales with moment-to-moment fluctuations in the organism's rotational speed (Fisher et al. 2022); thus, their activity should jump whenever the animal executes a saccadic turn (Geurten et al. 2014). Importantly, pairing dopamine neuron activity with a visual cue persistently strengthens the cue's influence on head direction cells, whereas inhibiting these specific dopamine neurons decreases the influence of a visual cue (Fisher et al. 2022). Together, these results argue that dopamine specifically accelerates ER→EPG synaptic plasticity during rotational moments. Rotational movements are special for the head direction system because they provide a stream of new data for the head direction system. This allows learning rates to be low at other times, which should prevent overlearning of head directions that are oversampled. This modulation is important, because goal-directed locomotion often involves fixing a particular head direction for a prolonged period, thereby creating a biased sample of the sensory world (**Figure 3a**).

Indeed, in a computational model of the head direction system, performance is improved by linking the rate of Hebbian plasticity to the animal's rotational speed (Fisher et al. 2022, Kim et al. 2019) (**Figure 3b**). This adaptive learning rate ensures that learning only occurs when new information is available. Without an adaptive learning rate, the network learns a biased pattern of ER→EPG weights because the sample of gaze directions is biased. Essentially, there is a conflict between the animal's need to perform a goal-directed action (which limits the range of experiences) and its need to engage in statistical learning (which requires broad sampling of experiences). Dopamine resolves this conflict by compressing learning into epochs of data-rich exploration. Many mammalian dopamine neurons are also locked to specific kinematic features of motor performance (Barter et al. 2015, Engelhard et al. 2019, Hughes et al. 2020), and so perhaps they serve a similar function by compressing synaptic plasticity into epochs when task-specific movements are generating rich data sets for statistical learning.

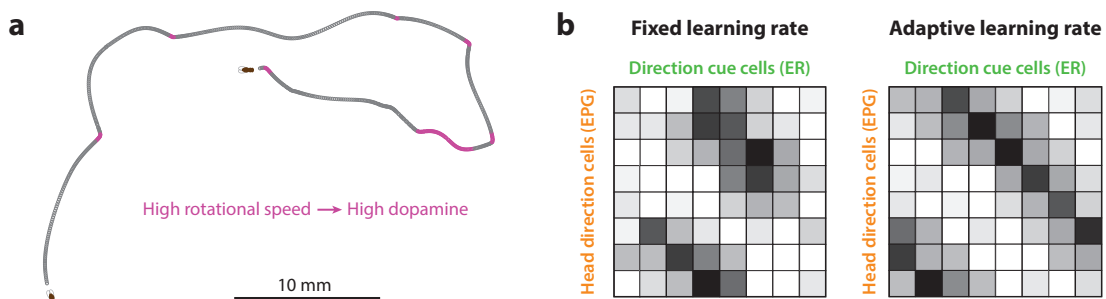


Figure 3

Learning at the right time. (a) An example locomotor trajectory of a fly walking in a virtual reality environment. Straight path segments are often separated by moments of high rotational speed. Similar paths are observed in free-walking *Drosophila* (Geurten et al. 2014). High rotational speed drives dopamine release in the head direction system, which accelerates Hebbian plasticity. (b) If the learning rate in a model is fixed, ER→EPG connection weights are disorderly, with certain head directions overrepresented and others underrepresented. If learning rate is adaptive (scaled with the organism's rotational speed), connection weights form an orderly stripe, with minimal biases. Locomotor trajectory in panel a provided by Wenyi Zhang; matrices in panel b are simplified schematics based on data and computational models from Fisher et al. (2022) and Kim et al. (2019).

Studies of arthropod navigation behavior provide more evidence that learning can be compressed into specific epochs. For example, dung beetles stand on their dung ball and rotate in place to memorize a snapshot of the world before embarking on a trip (el Jundi et al. 2016). Similarly, when a social insect first leaves its nest, it generally performs a tight circle around the nest, or else it locomotes out and back with a tight hairpin turn (Collett & Zeil 2018). These rotational movements are good ways to rapidly acquire an unbiased sample of the environment—while also injecting dopamine into the brain’s map of head direction.

BEYOND HEAD DIRECTION

Primary head direction neurons (EPG neurons) project from the ellipsoid body to a brain region called the protocerebral bridge (**Figure 1a**). There they send most of their output to a distinctive type of local neuron, called $\Delta 7$ (Wolff et al. 2015). Individual EPG neurons project to two separate locations in the protocerebral bridge; as a result, the protocerebral bridge contains two adjacent linearized maps of head direction (**Figure 4a**). Analysis of connectome data shows that EPG \rightarrow $\Delta 7$ connections are arranged so as to reformat the bump of activity into a sinusoidal spatial pattern (Hulse et al. 2021). Thus, the output of $\Delta 7$ cells can be treated as two spatial cycles of a sinusoidal pattern, whose phase represents head direction (**Figure 4b**).

This arrangement has two interesting implications. First, it provides a way to create any arbitrary phase shift in downstream neurons by simply plugging a shifted segment of the $\Delta 7$ map into that downstream population. Different downstream populations can sample different phase shifts (**Figure 4a,b**).

Second, a sinusoidal spatial pattern of neural activity enables neural networks to perform vector addition. We can interpret each of these sinusoidal patterns of neural activity as a vector (**Figure 4c**), and adding two of these sinusoidal spatial patterns is equivalent to performing vector addition (Touretzky et al. 1993, Wittmann & Schwegler 1995). Thus, the transformation of the head direction representation in the protocerebral bridge allows networks downstream from the head direction system to easily perform vector computations (Stone et al. 2017).

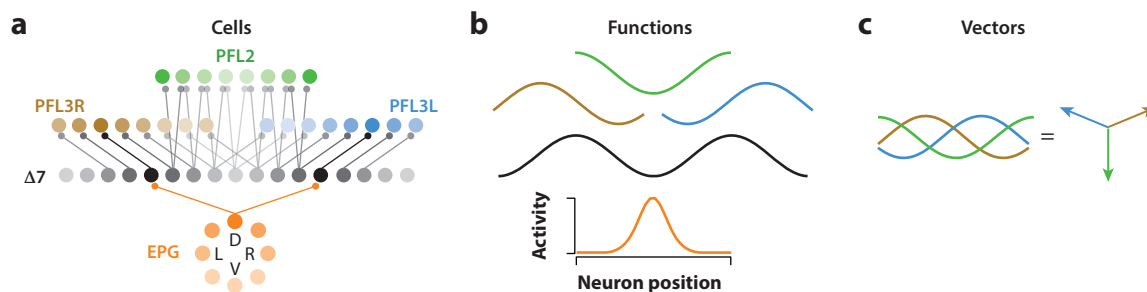
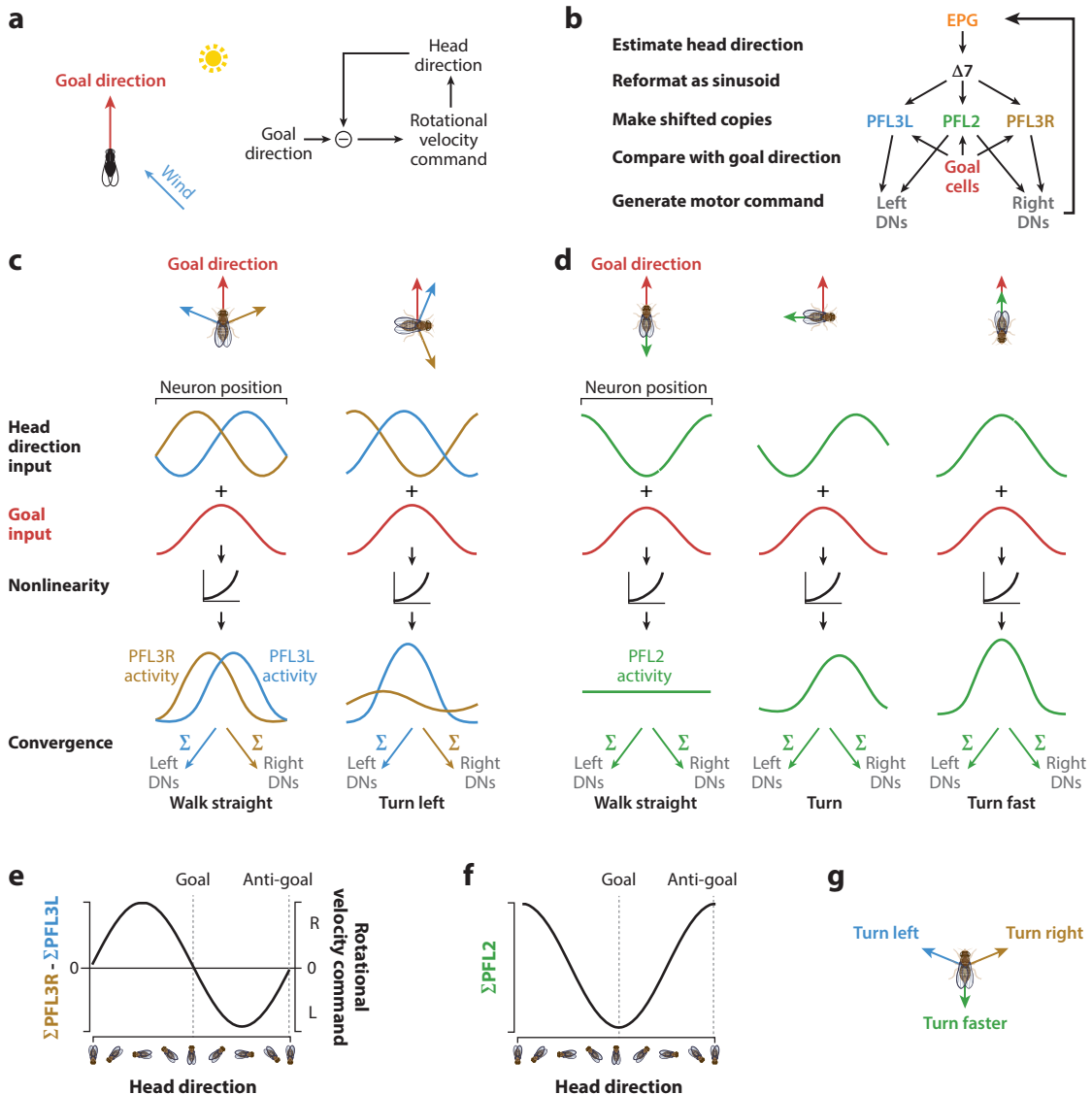


Figure 4

Reformatting the head direction representation. (a) EPG neurons form a circular topographic map of head direction in the *Drosophila* ellipsoid body. Individual EPG neurons project to two locations in the protocerebral bridge; these projections are shown here for just one EPG neuron. As a result, $\Delta 7$ cells form two side-by-side linearized maps of head direction in the protocerebral bridge. Each population of downstream neurons (e.g., the population of brown cells) extracts a complete copy of the $\Delta 7$ head direction map but with a shifted phase. Different downstream populations have different phase shifts. Here, three downstream populations are depicted, but there are many more downstream cell types (Hulse et al. 2021). (b) Each pattern of population activity can be represented as a continuous function over space. Whereas the bump of activity in EPG cells approximates a von Mises function (a normal distribution over a circular variable), the bump of activity in downstream neurons has a sinusoidal shape. (c) A sinusoid with a fixed spatial period can be interpreted as a vector, where the phase represents the direction of the vector, and the amplitude represents the magnitude of the vector.

STEERING

A key function of the head direction system is to guide steering. Many studies have shown that the activity of central complex neurons can predict and influence upcoming steering maneuvers (Green et al. 2019, Martin et al. 2015, Mussells Pires et al. 2022, Rayshubskiy et al. 2020, Shiozaki et al. 2020, Westeinde et al. 2022). However, the head direction system is not required for all steering per se. When EPG neurons are perturbed, *Drosophila* are still able to steer straight toward a cue; however, they lose the ability to perform menotaxis—that is, they can no longer maintain a fixed bearing in an arbitrary direction relative to environmental cues (Giraldo et al. 2018, Green et al. 2019) (**Figure 5a**). This argues that the head direction system is specifically required for navigation toward an internal goal held in memory.



(Caption appears on following page)

Figure 5 (Figure appears on preceding page)

Steering toward an internal goal. (a) To navigate straight toward a goal held in memory (such as a distant remembered feeding site or refuge), the brain must define a goal direction, which is anchored to environmental cues such as the sun and the wind. The brain must continuously estimate head direction relative to these cues and then compare the current head direction with the goal direction. (b) Key cell types and transformations in steering control. It is likely that there are multiple sets of goal cells. Descending neurons (DNs) project from the brain down to the ventral cord. (c) Model: each PFL3 population adds its head direction input with goal input; this sum is then passed through a nonlinearity. When head direction is aligned with the goal, total activity is equal in the two PFL3 populations. But when head direction is misaligned with the goal, this produces an asymmetry in the total activity of the two PFL3 populations and thus an appropriate turning command. This is because the head direction representation in each PFL3 population is shifted (*blue and brown arrows*); these representations are compared with the goal direction (*red arrow*). By definition, PFL3L neurons project to DNs on the left, and PFL3R neurons project to DNs on the right. (d) PFL2 neurons also combine head direction input with goal input; this sum is then passed through a nonlinearity. The green arrow represents the PFL2 head direction representation. Total PFL2 activity is minimal when head direction is aligned with the goal (*red arrow*) and maximal when the head direction is aligned with the antigoal. (e) The difference between total PFL3R activity and total PFL3L activity, plotted versus head direction. This function represents a dynamical system with two fixed points (*dashed lines*): One is stable (the goal) and the other is unstable (the antigoal). (f) Total PFL2 activity versus head direction. (g) Head direction signals in each PFL population represented as vectors. Each population detects when its head direction signal overlaps with the goal direction; this overlap drives the appropriate motor response. Figure based on data and models from Mussells Pires et al. (2022) and Westeinde et al. (2022).

It is important to realize that navigation toward an internal goal requires feedback. For example, humans trying to travel in a straight line cannot do so without feedback (Souman et al. 2009), and the same is true of arthropods (Barth & Seyfarth 1971, Khaldy et al. 2019). Without feedback, any organism or vehicle will inevitably drift off course. To maintain a fixed bearing, it is necessary to continually compare the current travel direction with an internal goal direction and to issue turning commands whenever there is a mismatch between these values (**Figure 5a**).

Moreover, the dynamics of neural activity in the head direction system match what we would expect from a feedback controller. The EPG activity bump rests in a stable position during internally guided straight-line navigation (Giraldo et al. 2018, Green et al. 2019). When the experimenter abruptly rotates the pattern of direction cues, this causes the EPG bump to move (Green et al. 2019, Seelig & Jayaraman 2015), evoking a corrective behavioral turn that returns the EPG bump to its original stable position prior to the cue shift (Green et al. 2019, Rayshubskiy et al. 2020). These dynamics imply that there are networks downstream from EPG neurons that compare the position of the EPG bump with an internal goal position. In essence, the problem of maintaining a fixed bearing becomes a problem of holding the EPG bump in a fixed position.

How does this work? Steering during walking depends on descending neurons that project from the brain to the leg control regions of the ventral cord. Specifically, the right-left difference in the activity of these descending neurons influences the organism's upcoming rotational velocity (Rayshubskiy et al. 2020). The output layer of the head direction system (consisting of $\Delta 7$ neurons) is connected to these steering descending neurons via three interposed cell types: PFL2, PFL3R, and PFL3L (**Figure 5b**). PFL3R and PFL3L neurons project to descending neurons on the right and left; these cells drive right and left turning, respectively (Mussells Pires et al. 2022). Meanwhile, each PFL2 cell projects bilaterally; these cells drive increases in rotational speed, regardless of turning direction (Westeinde et al. 2022). PFL activity depends on the relationship between head direction and goal direction, because each PFL population receives a shifted head direction map from $\Delta 7$ neurons (**Figure 4a**) as well as input from goal cells (Mussells Pires et al. 2022, Westeinde et al. 2022) (**Figure 5b**). The goal is represented as a static sinusoidal pattern of neural activity over the goal cell population. When head direction and goal are aligned, there is equal total activity in the PFL3R and PFL3L populations (**Figure 5c**), and PFL2 activity is minimal (**Figure 5d**). But when heading and goal are misaligned, PFL3 activity becomes asymmetric (**Figure 5c**), and PFL2 activity increases (**Figure 5d**), driving compensatory turning.

In essence, PFL2/3 cells transform an allocentric head direction map into an egocentric steering command. They do this by comparing the current allocentric head direction representation with an allocentric representation of the goal. Any mismatch between these quantities then triggers an egocentric rotational velocity command. PFL3 neurons specify the direction of the turn, whereas PFL2 neurons increase the vigor of the turn (Mussells Pires et al. 2022, Westeinde et al. 2022) (**Figure 5e–g**).

SELECTING AND STORING A GOAL

Recent models argue that goal signals should be stored as spatial sinusoids in the fan-shaped body, with the phase of the sinusoid corresponding to the direction of the goal (Dan et al. 2022, Mussells Pires et al. 2022, Stone et al. 2017, Westeinde et al. 2022). In principle, goals could be stored as sinusoidal patterns of persistent neural activity or as sinusoidal spatial patterns of synaptic weights (Goulard et al. 2021). Several studies have identified several populations of candidate goal cells in the fan-shaped body, all directly or indirectly presynaptic to PFL cells (Matheson et al. 2022, Mussells Pires et al. 2022). PFL cells receive input from a remarkably large number of cell types in the fan-shaped body (Hulse et al. 2021), and so it seems likely that there are in fact many types of goal cells. This architecture suggests a mechanism for holding multiple goals in memory. In each goal cell population, the amplitude of activity can fluctuate over time, representing the changing salience of that goal (Matheson et al. 2022, Mussells Pires et al. 2022), with resulting changes in PFL population dynamics (Westeinde et al. 2022).

Logically, the choice of a goal should depend on the expectation of reward. Thus, it has been proposed that the process of selecting a goal involves the brain's reinforcement learning networks in the mushroom body (Collett & Collett 2018, Webb & Wystrach 2016). The mushroom body provides indirect anatomical input to PFL3 neurons via cells in the fan-shaped body (Hulse et al. 2021, Li et al. 2020), and in ants, internally guided navigation is disrupted by mushroom body perturbations (Buehlmann et al. 2020, Kamhi et al. 2020). It has been suggested that the association between head directions and reward expectation signals serves to initialize a new goal direction (Dan et al. 2022, Goulard et al. 2021, Matheson et al. 2022).

If the head direction representation shifts to a new coordinate frame, the goal representation would need to shift accordingly. For example, if the phase of the head direction representation drifts by 90° , then the phase of the goal representation would need to move by 90° as well. In the future, it will be interesting to understand how the brain might enforce an alignment between these neural codes.

TRANSLATIONAL VELOCITY

Any autonomous vehicle or biological navigation system needs a speedometer as well as a compass. Indeed, there is clear evidence that the arthropod brain takes the organism's speed into account when organizing navigation (Ronacher & Wehner 1995, Schöne 1996, Srinivasan et al. 1996). Accordingly, we would expect to find neurons in the brain that monitor the speed of forward movement.

Importantly, however, not all locomotor movements are forward. For example, ants and dung beetles can navigate for long distances while walking backward. Remarkably, their navigation system can account for this, allowing them to maintain a straight path even as they switch between forward and backward walking (Dacke et al. 2021, Pfeffer & Wittlinger 2016). To take another example, flying insects often move sideways because they are being carried on the wind. Again, remarkably, the brain's navigation system can account for this, allowing them to maintain their desired path (Riley et al. 1999). These examples argue that the brain has access to the direction of egocentric translation (forward/backward, left/right). These directional movement signals likely

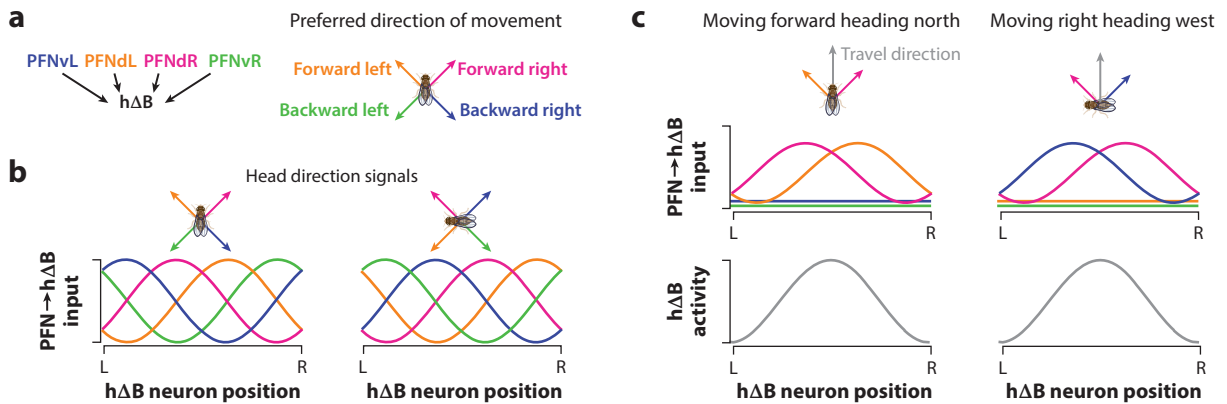


Figure 6

Transforming representations of movement from egocentric to allocentric coordinates. (a) Four PFN types converge onto hΔB neurons in the fan-shaped body. The activity of each type scales with the organism's translational velocity in its preferred egocentric direction. (b) Each PFN type also receives a copy of the head direction representation from Δ7 neurons. These head representations become inputs to hΔB neurons, with the indicated phase shifts. These are performed by the wiring pattern of the Δ7→PFN→hΔB pathway. Here, each sinusoid shows the input provided by one PFN type to the entire hΔB population; for visualization in this schematic, all four sinusoids are scaled to the same amplitude to enable comparison of their phases; in reality, however, all four PFN types are never coactive. When the organism rotates left, the phases of all these sinusoids shift to the right. (c) The hΔB representation of northward travel is the same, regardless of whether the organism is moving forward while heading north or moving right while heading west. Thus, hΔB neurons form a vector velocity representation of the organism's travel, invariant to head direction.

come from optic flow (Ronacher & Wehner 1995, Schöne 1996, Srinivasan et al. 1996) along with proprioception and/or motor-efference copy (Wittlinger et al. 2007). All these directional movement signals are transposed from egocentric to allocentric coordinates for effective navigation (Bicanski & Burgess 2020).

Recent studies in bees and *Drosophila* have revealed how this computation is implemented (Lu et al. 2021, Lyu et al. 2021, Stone et al. 2017). These studies found a Cartesian system for tracking translational velocity in egocentric coordinates. This system consists of four PFN cell types, each tuned to a different egocentric direction of movement (Figure 6a). These PFN neurons track the animal's egocentric velocity by fusing optic flow signals with nonvisual inputs, probably proprioception and motor efference. Activity in each PFN type scales with velocity in its preferred direction. At the same time, each PFN type also receives a complete map of head direction from Δ7 neurons (Figure 6b). Together, all four PFN types collectively prefer all possible combinations of head direction and egocentric movement direction.

At the next network layer, PFN neurons synapse onto hΔB neurons. These connections are shifted so as to combine signals from PFN neurons with the same preferred allocentric travel direction. As a result, hΔB neurons acquire a representation of allocentric travel direction that is invariant to head direction (Lu et al. 2021, Lyu et al. 2021). For example, at the level of hΔB neurons, moving forward while facing north is the same as moving right while heading west (Figure 6c). Meanwhile, the amplitude of the hΔB bump scales with the forward component of the animal's speed.

Abstractly, we can think of the four PFN types as four vectors, all linked to the head direction system (Figure 6b). The scale of each vector depends on the animal's egocentric direction and speed. The hΔB population adds these four vectors together by summing across four sinusoidal spatial patterns (Figure 6c). The resulting pattern of hΔB population activity is also a sinusoid, with a phase that represents allocentric travel direction and an amplitude that represents speed.

There are many other PFN types in the central complex beyond the PFN neurons that are presynaptic to h Δ B cells (Hulse et al. 2021, Sayre et al. 2021, Wolff & Rubin 2018). Each PFN type is anatomically positioned to combine an allocentric direction map with some sort of egocentric vector signal. Moreover, each PFN type has a distinctive pattern of shifted inputs and outputs, analogous to the arrangement of $\Delta 7 \rightarrow \text{PFN} \rightarrow \text{h}\Delta\text{B}$ connections. Thus, it seems likely that different PFN types are involved in different sorts of spatial coordinate transformations via vector addition and subtraction. For example, some may be involved in transforming between body-centric and head-centric coordinates or analyzing the relationship between different coordinate frames (Currier et al. 2020, Hulse et al. 2021).

PATH INTEGRATION

Path integration is the process by which an animal tracks its velocity over time to form a running estimate of its position in space. Many social insects—such as ants, bees, and wasps—integrate their translational velocity over time to help guide their return to their nest site after a foraging trip (Collett 2019, Heinze et al. 2018). The behavior of these insects tells us that they must be tracking the net distance and direction of their trip. This is often called a path integral, but it might make more sense to call it a path vector to emphasize that it has direction as well as magnitude. This stored path vector is used to guide the insect back toward its nest.

Although *Drosophila* do not build nests, recent studies have revealed that they are capable of path integration (Brockmann et al. 2018, Kim & Dickinson 2017). When a hungry fly encounters a morsel of food, it feeds for a time before walking away. If the fly walks around without finding more food, it will often return to the former feeding site, and if it does not find the food there, it will execute a local search. Optogenetic virtual food can be substituted for real food in this paradigm, giving the experimenter tight control over the location and timing of food encounters (Behbahani et al. 2021, Corfas et al. 2019, Titova et al. 2022). Importantly, these experiments are performed in darkness; thus, the only available inputs to the path integrator are probably proprioceptive cues and/or motor efference copy.

Many models of path integration have been proposed, operating in different coordinate frames (Vickerstaff & Cheung 2010). A major step toward resolving this debate came from the recent discovery of an allocentric phasor representation of the travel velocity vector in h Δ B neurons (Lu et al. 2021, Lyu et al. 2021). It seems likely that h Δ B neurons lie upstream of the integration step because path integration is disrupted when the PFN \rightarrow h Δ B pathway is perturbed (Lu et al. 2021). Based on these results, it seems likely that the path vector (similar to the travel vector) is represented as an allocentric phasor.

Importantly, an organism's estimate of its position does not depend on path integration alone; it also depends on local landmarks along the path. For example, ants can stick to a familiar path using remembered local landmarks as well as path integration (Müller & Wehner 2010, Narendra 2007). Bees can learn to associate points along the path vector with specific local objects (Srinivasan et al. 1999). Given this, it makes sense that the path vector should be encoded in allocentric coordinates, because it needs to be integrated with information about local object positions in the world.

How is the path vector stored? Most models assume a persistent graded change in firing rates (Stone et al. 2017, Vickerstaff & Di Paolo 2005, Wittmann & Schwegler 1995). However, in ants, the path vector is relatively stable for a day or two (Cheng et al. 2005, Ziegler & Wehner 1997), and a persistent graded change in firing rate seems implausible on this timescale.

A second possibility is that the path vector is stored via a set of ring attractors, one for each compass direction. The distance traveled in each direction would be represented by the position of the activity bump in the corresponding ring (Burak & Fiete 2009, Samsonovich & McNaughton

1997). However, this implementation has not been seriously considered in arthropods because it would require a large number of cells.

A third possibility is that the path vector is stored via changes in synaptic weights. Again, this implementation had not been seriously considered until recently (Hulse et al. 2021). However, if the head direction system can reorganize its internal weights over a timescale of minutes, it is not clear why the path integration system could not do the same.

Whatever the storage mechanism(s), the path vector needs to be rezeroed intermittently. In hungry flies, path integration can be rezeroed by an encounter with a food stimulus. In an extended patch containing multiple virtual (optogenetic) discrete food objects, the path vector is rezeroed at the center of the patch, even if there is no virtual food object in that particular location (Behbahani et al. 2021). This observation suggests that the brain estimates the spatial gradient of expected value over the environment and that the path integration mechanism is rezeroed around the maximum of that gradient. Thus, rezeroing the path vector may be related to the phenomenon of place preference learning (Melnattur et al. 2021, Ofstad et al. 2011): In both cases, the brain seems to be learning an association between spatial location and expected value. These forms of learning might involve the bidirectional connections between the central complex and the brain's reinforcement learning centers (Hulse et al. 2021, Li et al. 2020).

Importantly, navigation via path integration involves read/write memory: The path vector must be written (remembered) and also read out (retrieved) to guide navigation. Thus, the mechanisms of path integration must converge with mechanisms of steering control. This process becomes more complicated if the brain needs to write (and read out) multiple path vectors, as suggested by experiments in bees (Dacke & Srinivasan 2008).

OUTLOOK

It is generally assumed that working memory is stored in patterns of persistent neural activity, whereas long-term memory is stored in patterns of synaptic weights. In this review, I have argued for a different view—namely, that both types of processes are continually at work. Biological attractor networks can maintain patterns of persistent activity that store key variables in memory; at the same time, the pattern of functional connections in these attractor networks is constantly changing via Hebbian learning rules interacting with sensory feedback and attractor dynamics, all under the control of neuromodulatory systems. At the moment, there is strong evidence for synaptic plasticity at just one site in the central complex [ER→EPG synapses (Fisher et al. 2019, 2022; Kim et al. 2019)], but it seems likely that there are other sites as well. For example, there is some evidence that body size estimates are calibrated by synaptic plasticity in the protocerebral bridge (Krause et al. 2019). It has been suggested that angular velocity integration in the head direction system is calibrated by plasticity at the synapses from velocity-direction cells onto head direction cells (Vafidis et al. 2022). Moreover, it has been proposed that flexible goal switching is accomplished by plasticity at synapses onto steering drive cells, that is, PFL3 neurons (Gouldard et al. 2021). Finally, it has been suggested that path integration is implemented via synaptic plasticity at sites downstream from h Δ B neurons (Hulse et al. 2021). Testing these hypotheses will not be easy because we cannot directly observe synaptic weights *in vivo*. However, we can generally infer something about the synaptic weights in a network by comparing pre- and postsynaptic dynamics, and we may be able to manipulate plasticity by manipulating neuromodulatory systems (Fisher et al. 2022). We can also incorporate Hebbian learning rules into connectome-constrained network models (Litwin-Kumar & Turaga 2019) to help us understand how synaptic plasticity can change network output.

More generally, arthropod navigation networks provide an excellent opportunity to investigate the neural implementation of basic computations with broad relevance to all organisms.

Arthropods have already revealed the implementation of ring attractor dynamics (Green et al. 2017, Kim et al. 2017, Turner-Evans et al. 2017) and coordinate transformations (Lu et al. 2021, Lyu et al. 2021). Beyond this, arthropod studies have illuminated fundamental areas of systems neuroscience, including visual motion detection via correlation (Reichardt 1961), central pattern generators (Hughes & Wiersma 1960, Wilson 1961), circadian rhythm generation (Dubowy & Sehgal 2017), histogram equalization in image processing (Laughlin 1981), predictive coding (Srinivasan et al. 1982), dimensionality expansion (Laurent 2002, Litwin-Kumar et al. 2017, Stevens 2015), divisive normalization (Luo et al. 2010, Olsen et al. 2010), integral feedback control (Schnell et al. 2014), and path integration (Heinze et al. 2018). Importantly, navigation requires an organism to engage with its physical environment. Therefore, the study of navigation encourages us to think of neural systems as embodied control systems—not disembodied systems for symbolic manipulation. It seems likely that the demands of embodiment have profoundly shaped the evolution and development of these neural control systems (de Croon et al. 2022). The problems faced by any navigating animal or vehicle are fundamentally similar because the problems inherent in navigation are universal problems of geometry and physics. With the advent of complete connectomes that span the entire arthropod nervous system, we should be able to build artificial neural networks that emulate biological neural networks—not just abstractly, but in detail. This is an important step toward a unified understanding of the design and control principles underlying intelligent autonomous control systems, both artificial and biological.

DISCLOSURE STATEMENT

The author is not aware of any affiliations, memberships, funding, or financial holdings that might be perceived as affecting the objectivity of this review.

ACKNOWLEDGMENTS

I am grateful for many useful conversations with Michael Dickinson, Shaul Druckmann, Jan Drugowitch, and many colleagues in my own lab.

LITERATURE CITED

- Ajabi Z, Keinath AT, Wei X-X, Brandon MP. 2021. Population dynamics of the thalamic head direction system during drift and reorientation. *bioRxiv* 2021.08.30.458266. <https://doi.org/10.1101/2021.08.30.458266>
- Arendse MC, Kruyswijk CJ. 1981. Orientation of *Talitrus saltator* to magnetic fields. *Neth. J. Sea Res.* 15:23–32
- Barter JW, Li S, Lu D, Bartholomew RA, Rossi MA, et al. 2015. Beyond reward prediction errors: the role of dopamine in movement kinematics. *Front. Integr. Neurosci.* 9:39
- Barth FG, Seyfarth E-A. 1971. Slit sense organs and kinesthetic orientation. *Z. Vergl. Physiol.* 74:326–28
- Bates AS, Janssens J, Jefferis GS, Aerts S. 2019. Neuronal cell types in the fly: single-cell anatomy meets single-cell genomics. *Curr. Opin. Neurobiol.* 56:125–34
- Beetz MJ, Kraus C, Franzke M, Dreyer D, Strube-Bloss MF, et al. 2021. Flight-induced compass representation in the monarch butterfly heading network. *Curr. Biol.* 32:338–49.e5
- Behbahani AH, Palmer EH, Corfas RA, Dickinson MH. 2021. *Drosophila* re-zero their path integrator at the center of a fictive food patch. *Curr. Biol.* 31:4534–46.e5
- Bell WJ, Kramer E. 1979. Search and anemotactic orientation of cockroaches. *J. Insect Physiol.* 25:631–40
- Bicanski A, Burgess N. 2020. Neuronal vector coding in spatial cognition. *Nat. Rev. Neurosci.* 21:453–70
- Böhm H. 1995. Dynamic properties of orientation to turbulent air current by walking carrion beetles. *J. Exp. Biol.* 198:1995–2005
- Böhm H, Heinzel H-G, Scharstein H, Wendler G. 1991. The course control system of beetles walking in an air-current field. *J. Comp. Physiol. A* 169:671–83

- Boles LC, Lohmann KJ. 2003. True navigation and magnetic maps in spiny lobsters. *Nature* 421:60–63
- Brockmann A, Basu P, Shakeel M, Murata S, Murashima N, et al. 2018. Sugar intake elicits intelligent searching behavior in flies and honey bees. *Front. Behav. Neurosci.* 12:280
- Buehlmann C, Wozniak B, Goulard R, Webb B, Graham P, Niven JE. 2020. Mushroom bodies are required for learned visual navigation, but not for innate visual behavior, in ants. *Curr. Biol.* 30:3438–43.e2
- Burak Y, Fiete IR. 2009. Accurate path integration in continuous attractor network models of grid cells. *PLOS Comput. Biol.* 5:e1000291
- Cheng K, Narendra A, Wehner R. 2005. Behavioral ecology of odometric memories in desert ants: acquisition, retention, and integration. *Behav. Ecol.* 17:227–35
- Cheng K, Shettleworth SJ, Huttenlocher J, Rieser JJ. 2007. Bayesian integration of spatial information. *Psychol. Bull.* 133:625–37
- Cohn R, Morante I, Ruta V. 2015. Coordinated and compartmentalized neuromodulation shapes sensory processing in *Drosophila*. *Cell* 163:1742–55
- Collett M, Collett TS. 2018. How does the insect central complex use mushroom body output for steering? *Curr. Biol.* 28:R733–34
- Collett TS. 2019. Path integration: how details of the honeybee waggle dance and the foraging strategies of desert ants might help in understanding its mechanisms. *J. Exp. Biol.* 222:jeb205187
- Collett TS, Zeil J. 2018. Insect learning flights and walks. *Curr. Biol.* 28:R984–88
- Cope AJ, Sabo C, Vasilaki E, Barron AB, Marshall JA. 2017. A computational model of the integration of landmarks and motion in the insect central complex. *PLOS ONE* 12:e0172325
- Corfas RA, Sharma T, Dickinson MH. 2019. Diverse food-sensing neurons trigger idiothetic local search in *Drosophila*. *Curr. Biol.* 29:1660–68.e4
- Currier TA, Matheson AM, Nagel KI. 2020. Encoding and control of orientation to airflow by a set of *Drosophila* fan-shaped body neurons. *eLife* 9:e61510
- Dacke M, Baird E, Byrne M, Scholtz CH, Warrant EJ. 2013. Dung beetles use the Milky Way for orientation. *Curr. Biol.* 23:298–300
- Dacke M, Baird E, el Jundi B, Warrant EJ, Byrne M. 2021. How dung beetles steer straight. *Annu. Rev. Entomol.* 66:243–56
- Dacke M, Bell ATA, Foster JJ, Baird EJ, Strube-Bloss MF, et al. 2019. Multimodal cue integration in the dung beetle compass. *PNAS* 116:14248–53
- Dacke M, Byrne MJ, Scholtz CH, Warrant EJ. 2004. Lunar orientation in a beetle. *Proc. Biol. Sci.* 271:361–65
- Dacke M, Srinivasan MV. 2008. Two odometers in honeybees? *J. Exp. Biol.* 211:3281–86
- Dan C, Kappagantula R, Hulse BK, Jayaraman V, Hermundstad AM. 2022. Flexible control of behavioral variability mediated by an internal representation of head direction. *bioRxiv* 2021.08.18.456004. <https://doi.org/10.1101/2021.08.18.456004>
- de Croon GCHE, Dupeyroux JJG, Fuller SB, Marshall JAR. 2022. Insect-inspired AI for autonomous robots. *Sci. Robot.* 7:eab16334
- Dickinson MH. 2014. Death Valley, *Drosophila*, and the Devonian toolkit. *Annu. Rev. Entomol.* 59:51–72
- Dubowy C, Sehgal A. 2017. Circadian rhythms and sleep in *Drosophila melanogaster*. *Genetics* 205:1373–97
- el Jundi B, Foster JJ, Byrne MJ, Baird E, Dacke M. 2015a. Spectral information as an orientation cue in dung beetles. *Biol. Lett.* 11:20150656
- el Jundi B, Foster JJ, Khaldy L, Byrne MJ, Dacke M, Baird E. 2016. A snapshot-based mechanism for celestial orientation. *Curr. Biol.* 26:1456–62
- el Jundi B, Warrant EJ, Byrne MJ, Khaldy L, Baird E, et al. 2015b. Neural coding underlying the cue preference for celestial orientation. *PNAS* 112:11395–400
- Engelhard B, Finkelstein J, Cox J, Fleming W, Jang HJ, et al. 2019. Specialized coding of sensory, motor and cognitive variables in VTA dopamine neurons. *Nature* 570:509–13
- Fisher YE, Lu J, D'Alessandro I, Wilson RI. 2019. Sensorimotor experience remaps visual input to a heading-direction network. *Nature* 576:121–25
- Fisher YE, Marquis M, D'Alessandro I, Wilson RI. 2022. Dopamine promotes head direction plasticity during orienting movements. *Nature* 612:316–22
- Fleischmann PN, Grob R, Müller VL, Wehner R, Rössler W. 2018. The geomagnetic field is a compass cue in *Cataglyphis* ant navigation. *Curr. Biol.* 28:1440–44.e2

- Franconville R, Beron C, Jayaraman V. 2018. Building a functional connectome of the *Drosophila* central complex. *eLife* 7:e37017
- Frémaux N, Gerstner W. 2015. Neuromodulated spike-timing-dependent plasticity, and theory of three-factor learning rules. *Front. Neural Circuits* 9:85
- Geurten BRH, Jähde P, Corthals K, Göpfert MC. 2014. Saccadic body turns in walking *Drosophila*. *Front. Behav. Neurosci.* 8:365
- Giraldo YM, Leitch KJ, Ros IG, Warren TL, Weir PT, Dickinson MH. 2018. Sun navigation requires compass neurons in *Drosophila*. *Curr. Biol.* 28:2845–52.e4
- Goulard R, Buehlmann C, Niven JE, Graham P, Webb B. 2021. A unified mechanism for innate and learned visual landmark guidance in the insect central complex. *PLOS Comput. Biol.* 17:e1009383
- Green J, Adachi A, Shah KK, Hirokawa JD, Magani PS, Maimon G. 2017. A neural circuit architecture for angular integration in *Drosophila*. *Nature* 546:101–6
- Green J, Vijayan V, Mussells Pires P, Adachi A, Maimon G. 2019. A neural heading estimate is compared with an internal goal to guide oriented navigation. *Nat. Neurosci.* 22:1460–68
- Grover D, Chen J-Y, Xie J, Li J, Changeux J-P, Greenspan RJ. 2022. Differential mechanisms underlie trace and delay conditioning in *Drosophila*. *Nature* 603:302–8
- Haberkern H, Chitnis SS, Hubbard PM, Goulet T, Hermundstad AM, Jayaraman V. 2022. Maintaining a stable head direction representation in naturalistic visual environments. *bioRxiv* 2022.05.17.492284. <https://doi.org/10.1101/2022.05.17.492284>
- Handler A, Graham TGW, Cohn R, Morante I, Siliciano AF, et al. 2019. Distinct dopamine receptor pathways underlie the temporal sensitivity of associative learning. *Cell* 178:60–75.e19
- Hardcastle BJ, Omoto JJ, Kandimalla P, Nguyen B-CM, Keleş MF, et al. 2021. A visual pathway for skylight polarization processing in *Drosophila*. *eLife* 10:e63225
- Heinze S, Homberg U. 2007. Maplike representation of celestial E-vector orientations in the brain of an insect. *Science* 315:995–97
- Heinze S, Homberg U. 2009. Linking the input to the output: new sets of neurons complement the polarization vision network in the locust central complex. *J. Neurosci.* 29:4911–21
- Heinze S, Narendra A, Cheung A. 2018. Principles of insect path integration. *Curr. Biol.* 28:R1043–58
- Heinze S, Reppert SM. 2011. Sun compass integration of skylight cues in migratory monarch butterflies. *Neuron* 69:345–58
- Heinzel H-G, Böhm H. 1989. The wind-orientation of walking carrion beetles. *J. Comp. Physiol. A* 164:775–86
- Hige T, Aso Y, Rubin GM, Turner GC. 2015. Plasticity-driven individualization of olfactory coding in mushroom body output neurons. *Nature* 526:258–62
- Homberg U. 2004. In search of the sky compass in the insect brain. *Naturwissenschaften* 91:199–208
- Homberg U. 2015. Sky compass orientation in desert locusts—evidence from field and laboratory studies. *Front. Behav. Neurosci.* 9:346
- Honkanen A, Adden A, da Silva Freitas J, Heinze S. 2019. The insect central complex and the neural basis of navigational strategies. *J. Exp. Biol.* 222(Suppl. 1):jeb188854
- Hughes GM, Wiersma CAG. 1960. The co-ordination of swimmeret movements in the crayfish, *Procambarus clarkii* (Girard). *J. Exp. Biol.* 37:657–70
- Hughes RN, Bakhurin KI, Petter EA, Watson GDR, Kim N, et al. 2020. Ventral tegmental dopamine neurons control the impulse vector during motivated behavior. *Curr. Biol.* 30:2681–94.e5
- Hulse BK, Haberkern H, Franconville R, Turner-Evans DB, Takemura S-Y, et al. 2021. A connectome of the *Drosophila* central complex reveals network motifs suitable for flexible navigation and context-dependent action selection. *eLife* 10:e66039
- Hulse BK, Jayaraman V. 2020. Mechanisms underlying the neural computation of head direction. *Annu. Rev. Neurosci.* 43:31–54
- Kamhi JF, Barron AB, Narendra A. 2020. Vertical lobes of the mushroom bodies are essential for view-based navigation in Australian *Myrmecia* ants. *Curr. Biol.* 30:3432–37.e3
- Khalidy L, Peleg O, Tocco C, Mahadevan L, Byrne M, Dacke M. 2019. The effect of step size on straight-line orientation. *J. R. Soc. Interface* 16:20190181
- Kim IS, Dickinson MH. 2017. Idiothetic path integration in the fruit fly *Drosophila melanogaster*. *Curr. Biol.* 27:2227–38.e3

- Kim SS, Hermundstad AM, Romani S, Abbott LF, Jayaraman V. 2019. Generation of stable heading representations in diverse visual scenes. *Nature* 576:126–31
- Kim SS, Rouault H, Druckmann S, Jayaraman V. 2017. Ring attractor dynamics in the *Drosophila* central brain. *Science* 356:849–53
- Knierim JJ, Zhang K. 2012. Attractor dynamics of spatially correlated neural activity in the limbic system. *Annu. Rev. Neurosci.* 35:267–85
- Krause T, Spindler L, Poeck B, Strauss R. 2019. *Drosophila* acquires a long-lasting body-size memory from visual feedback. *Curr. Biol.* 29:1833–41.e3
- Kutschireiter A, Basnak MA, Drugowitsch J. 2022. Bayesian inference in ring attractor networks. bioRxiv 2021.12.17.473253. <https://doi.org/10.1101/2021.12.17.473253>
- Labhart T, Meyer EP. 2002. Neural mechanisms in insect navigation: polarization compass and odometer. *Curr. Opin. Neurobiol.* 12:707–14
- Laughlin SB. 1981. A simple coding procedure enhances a neuron's information capacity. *Z. Naturforsch. C* 36:910–12
- Laurent G. 2002. Olfactory network dynamics and the coding of multidimensional signals. *Nat. Rev. Neurosci.* 3:884–95
- Li F, Lindsey JW, Marin EC, Otto N, Dreher M, et al. 2020. The connectome of the adult *Drosophila* mushroom body provides insights into function. *eLife* 9:e62576
- Liang X, Ho MCW, Zhang Y, Li Y, Wu MN, et al. 2019. Morning and evening circadian pacemakers independently drive premotor centers via a specific dopamine relay. *Neuron* 102:843–57.e4
- Litwin-Kumar A, Harris KD, Axel R, Sompolinsky H, Abbott LF. 2017. Optimal degrees of synaptic connectivity. *Neuron* 93:1153–64.e7
- Litwin-Kumar A, Turaga SC. 2019. Constraining computational models using electron microscopy wiring diagrams. *Curr. Opin. Neurobiol.* 58:94–100
- Lu J, Behbehani A, Hamburg L, Westeinde EA, Dawson PM, et al. 2021. Transforming representations of movement from body- to world-centric space. *Nature* 601:98–104
- Luo SX, Axel R, Abbott LF. 2010. Generating sparse and selective third-order responses in the olfactory system of the fly. *PNAS* 107:10713–18
- Lyu C, Abbott LF, Maimon G. 2021. Building an allocentric travelling direction signal via vector computation. *Nature* 601:92–97
- Martin JP, Guo P, Mu L, Harley CM, Ritzmann RE. 2015. Central-complex control of movement in the freely walking cockroach. *Curr. Biol.* 25:2795–803
- Matheson AMM, Lanz AJ, Medina AM, Licata AM, Currier TA, et al. 2022. A neural circuit for wind-guided olfactory navigation. *Nat. Commun.* 13:4613
- Melnattur K, Kirszenblat L, Morgan E, Militchin V, Sakran B, et al. 2021. A conserved role for sleep in supporting spatial learning in *Drosophila*. *Sleep* 44:zsaa197
- Mizumori SJ, Williams JD. 1993. Directionally selective mnemonic properties of neurons in the lateral dorsal nucleus of the thalamus of rats. *J. Neurosci.* 13:4015–28
- Müller M, Wehner R. 2007. Wind and sky as compass cues in desert ant navigation. *Naturwissenschaften* 94:589–94
- Müller M, Wehner R. 2010. Path integration provides a scaffold for landmark learning in desert ants. *Curr. Biol.* 20:1368–71
- Mussells Pires P, Abbott LF, Maimon G. 2022. Converting an allocentric goal into an egocentric steering signal. bioRxiv 2022.11.10.516026. <https://doi.org/10.1101/2022.11.10.516026>
- Narendra A. 2007. Homing strategies of the Australian desert ant *Melophorus bagoti*. II. Interaction of the path integrator with visual cue information. *J. Exp. Biol.* 210:1804–12
- Ofstad TA, Zuker CS, Reiser MB. 2011. Visual place learning in *Drosophila melanogaster*. *Nature* 474:204–7
- Okubo TS, Patella P, D'Alessandro I, Wilson RI. 2020. A neural network for wind-guided compass navigation. *Neuron* 107:924–40.e18
- Olsen SR, Bhandawat V, Wilson RI. 2010. Divisive normalization in olfactory population codes. *Neuron* 66:287–99
- Omoto JJ, Keles MF, Nguyen BM, Bolanos C, Lovick JK, et al. 2017. Visual input to the *Drosophila* central complex by developmentally and functionally distinct neuronal populations. *Curr. Biol.* 27:1098–110

- Page HJI, Walters DM, Knight R, Piette CE, Jeffery KJ, Stringer SM. 2014. A theoretical account of cue averaging in the rodent head direction system. *Philos. Trans. R. Soc. B* 369:20130283
- Pegel U, Pfeiffer K, Homberg U. 2018. Integration of celestial compass cues in the central complex of the locust brain. *J. Exp. Biol.* 221:jeb171207
- Pfeffer SE, Wittlinger M. 2016. How to find home backwards? Navigation during rearward homing of *Cataglyphis fortis* desert ants. *J. Exp. Biol.* 219:2119–26
- Pfeiffer K, Homberg U. 2007. Coding of azimuthal directions via time-compensated combination of celestial compass cues. *Curr. Biol.* 17:960–65
- Pfeiffer K, Kinoshita M, Homberg U. 2005. Polarization-sensitive and light-sensitive neurons in two parallel pathways passing through the anterior optic tubercle in the locust brain. *J. Neurophysiol.* 94:3903–15
- Rayshubskiy A, Holtz SL, D'Alessandro I, Li AA, Vanderbeck QX, et al. 2020. Neural circuit mechanisms for steering control in walking *Drosophila*. bioRxiv 2020.04.04.024703. <https://doi.org/10.1101/2020.04.04.024703>
- Reichardt W. 1961. Autocorrelation, a principle for evaluation of sensory information by the central nervous system. In *Sensory Communication*, ed. WA Rosenblith, pp. 303–17. Cambridge, MA: MIT Press
- Riley JR, Reynolds DR, Smith AD, Edwards AS, Osborne JL, et al. 1999. Compensation for wind drift by bumble-bees. *Nature* 400:126
- Ronacher BD, Wehner R. 1995. Desert ants *Cataglyphis fortis* use self-induced optic flow to measure distance travelled. *J. Comp. Physiol. A* 177:21–27
- Rumelhart DE, Hinton GE, Williams RJ. 1986. Learning representations by back-propagating errors. *Nature* 323:533–36
- Sakura M, Lambrinos D, Labhart T. 2008. Polarized skylight navigation in insects: model and electrophysiology of E-vector coding by neurons in the central complex. *J. Neurophysiol.* 99:667–82
- Samsonovich A, McNaughton BL. 1997. Path integration and cognitive mapping in a continuous attractor neural network model. *J. Neurosci.* 17:5900–20
- Sayre ME, Templin R, Chavez J, Kempenaers J, Heinze S. 2021. A projectome of the bumblebee central complex. *eLife* 10:e68911
- Schlegel P, Bates AS, Stürner T, Jagannathan SR, Drummond N, et al. 2021. Information flow, cell types and stereotypy in a full olfactory connectome. *eLife* 10:e66018
- Schnell B, Weir PT, Roth E, Fairhall AL, Dickinson MH. 2014. Cellular mechanisms for integral feedback in visually guided behavior. *PNAS* 111:5700–5
- Schöne H. 1996. Optokinetic speed control and estimation of travel distance in walking honeybees. *J. Comp. Physiol. A* 179:587–92
- Schöne H. 2014. *Spatial Orientation: The Spatial Control of Behavior in Animals and Man*. Princeton, NJ: Princeton Univ. Press
- Seelig JD, Jayaraman V. 2013. Feature detection and orientation tuning in the *Drosophila* central complex. *Nature* 503:262–66
- Seelig JD, Jayaraman V. 2015. Neural dynamics for landmark orientation and angular path integration. *Nature* 521:186–91
- Shiozaki HM, Ohta K, Kazama H. 2020. A multi-regional network encoding heading and steering maneuvers in *Drosophila*. *Neuron* 106:126–41.e5
- Skaggs WE, Knierim JJ, Kudrimoti HS, McNaughton BL. 1995. A model of the neural basis of the rat's sense of direction. *Adv. Neural Inf. Process. Syst.* 7:173–80
- Souman JL, Frissen I, Sreenivasa MN, Ernst MO. 2009. Walking straight into circles. *Curr. Biol.* 19:1538–42
- Srinivasan M, Zhang S, Lehrer M, Collett T. 1996. Honeybee navigation en route to the goal: visual flight control and odometry. *J. Exp. Biol.* 199:237–44
- Srinivasan MV, Laughlin SB, Dubs A. 1982. Predictive coding: a fresh view of inhibition in the retina. *Proc. R. Soc. Lond. B Biol. Sci.* 216:427–59
- Srinivasan MV, Zhang SW, Berry J, Cheng K, Zhu H. 1999. Honeybee navigation: linear perception of short distances travelled. *J. Comp. Physiol. A* 185:239–45
- Stevens CF. 2015. What the fly's nose tells the fly's brain. *PNAS* 112:9460–65
- Stone T, Webb B, Adden A, Weddig NB, Honkanen A, et al. 2017. An anatomically constrained model for path integration in the bee brain. *Curr. Biol.* 27:3069–85.e11

- Strausfeld NJ. 2012. *Arthropod Brains: Evolution, Functional Elegance, and Historical Significance*. Cambridge, MA: Harvard Univ. Press
- Sun Y, Nern A, Franconville R, Dana H, Schreiter ER, et al. 2017. Neural signatures of dynamic stimulus selection in *Drosophila*. *Nat. Neurosci.* 20:1104–13
- Taube JS. 1995. Head direction cells recorded in the anterior thalamic nuclei of freely moving rats. *J. Neurosci.* 15:70–86
- Taube JS, Muller RU, Ranck JB Jr. 1990a. Head-direction cells recorded from the postsubiculum in freely moving rats. I. Description and quantitative analysis. *J. Neurosci.* 10:420–35
- Taube JS, Muller RU, Ranck JB Jr. 1990b. Head-direction cells recorded from the postsubiculum in freely moving rats. II. Effects of environmental manipulations. *J. Neurosci.* 10:436–47
- Thoen HH, Marshall J, Wolff GH, Strausfeld NJ. 2017. Insect-like organization of the stomatopod central complex: functional and phylogenetic implications. *Front. Behav. Neurosci.* 11:12
- Titova AV, Kau BE, Tibor S, Mach J, Thang Vo-Doan T, et al. 2022. Displacement experiments provide evidence for path integration in *Drosophila*. bioRxiv 2022.07.22.501185. <https://doi.org/10.1101/2022.07.22.501185>
- Touretzky DS, Redish AD, Wan HS. 1993. Neural representation of space using sinusoidal arrays. *Neural Comput.* 5:869–84
- Turner-Evans D, Jensen KT, Ali S, Paterson T, Sheridan A, et al. 2020. The neuroanatomical ultrastructure and function of a biological ring attractor. *Neuron* 108:145–63.e10
- Turner-Evans D, Wegener S, Rouault H, Franconville R, Wolff T, et al. 2017. Angular velocity integration in a fly heading circuit. *eLife* 6:e23496
- Ugolini A, Chiussi R. 1996. Astronomical orientation and learning in the earwig *Labidura riparia*. *Behav. Processes* 36:151–61
- Vafidis P, Oswald D, D’Albis T, Kempter R. 2022. Learning accurate path integration in ring attractor models of the head direction system. *eLife* 11:e69841
- van Breugel F, Jewell R, Houle J. 2022. Active anemosensing hypothesis: how flying insects could estimate ambient wind direction through sensory integration and active movement. *J. R. Soc. Interface* 19:20220258
- Vickerstaff RJ, Cheung A. 2010. Which coordinate system for modelling path integration? *J. Theor. Biol.* 263:242–61
- Vickerstaff RJ, Di Paolo EA. 2005. Evolving neural models of path integration. *J. Exp. Biol.* 208:3349–66
- Warren TL, Giraldo YM, Dickinson MH. 2019. Celestial navigation in *Drosophila*. *J. Exp. Biol.* 222:jeb186148
- Watabe-Uchida M, Eshel N, Uchida N. 2017. Neural circuitry of reward prediction error. *Annu. Rev. Neurosci.* 40:373–94
- Webb B, Wystrach A. 2016. Neural mechanisms of insect navigation. *Curr. Opin. Insect Sci.* 15:27–39
- Westeinde EA, Kellogg E, Dawson PM, Lu J, Hamburg L, et al. 2022. Transforming a head direction signal into a goal-oriented steering command. bioRxiv 2022.11.10.516039. <https://doi.org/10.1101/2022.11.10.516039>
- Wilson DM. 1961. The central nervous control of flight in a locust. *J. Exp. Biol.* 38:471–90
- Wittlinger M, Wehner R, Wolf H. 2007. The desert ant odometer: a stride integrator that accounts for stride length and walking speed. *J. Exp. Biol.* 210:198–207
- Wittmann T, Schwegler H. 1995. Path integration—a network model. *Biol. Cybern.* 73:569–75
- Wolff T, Iyer NA, Rubin GM. 2015. Neuroarchitecture and neuroanatomy of the *Drosophila* central complex: a GAL4-based dissection of protocerebral bridge neurons and circuits. *J. Comp. Neurol.* 523:997–1037
- Wolff T, Rubin GM. 2018. Neuroarchitecture of the *Drosophila* central complex: a catalog of nodulus and asymmetrical body neurons and a revision of the protocerebral bridge catalog. *J. Comp. Neurol.* 526:2585–611
- Zhang K. 1996. Representation of spatial orientation by the intrinsic dynamics of the head-direction cell ensemble: a theory. *J. Neurosci.* 16:2112–26
- Ziegler PE, Wehner R. 1997. Time-courses of memory decay in vector-based and landmark-based systems of navigation in desert ants, *Cataglyphis fortis*. *J. Comp. Physiol. A* 181:13–20